

# A Unified View of DI- and ETD-FDTD Methods for Drude Media

José A. Pereda and Ana Grande

**Abstract**—A unified view of direct-integration (DI) and exponential-time-differencing (ETD) methods to incorporate Drude media, such as isotropic plasma and microwave graphene, into finite-difference time-domain (FDTD) simulators is provided. To this end, the Drude constitutive relation is expressed in integral form and the DI integrators are obtained by applying quadrature rules. Analogously, the ETD integrators are obtained by starting from the variation of constants formulae and applying the same quadrature rules as in the DI case. This approach allows one to directly compare the two families of methods. Additionally, the accuracy of each integrator is discussed and the stability condition of the resulting FDTD schemes is derived in exact closed-form by applying the von Neumann method.

**Index Terms**—Direct-integration methods, Drude media, exponential-time-differencing methods, finite-difference time-domain method, graphene, plasma.

## I. INTRODUCTION

The finite-difference time-domain (FDTD) method is one of the most popular numerical techniques for solving Maxwell’s equations in the time domain [1]. One of the first FDTD challenges was to include frequency dispersive materials within the simulations. Currently, there is a vast number of approaches to do it that fall into three groups: direct-integration (DI) methods [2], [3], recursive convolution (RC) techniques [4]-[7], and  $Z$ -transform methods [8], [9].

The DI methods are based on expressing the material constitutive relation as an auxiliary differential equation (ADE). This ADE is then discretized, term by term, by approximating derivatives with FDs. The DI techniques are also referred to as ADE or DI-ADE methods.

The exponential-time-differencing (ETD) methods can be included into the RC group. A review on ETD methods for first-order problems can be found in [10]. A comparison between some DI- and ETD-FDTD schemes for plasma problems was provided in [5], [11] and more recently in [12].

This communication provides a unified view of DI and ETD methods for Drude media, such as isotropic plasma and microwave graphene. Firstly, we introduce a systematic approach to derive DI methods. To this end, the constitutive relation is expressed in integral form and the DI integrators are obtained by applying quadrature rules. Then, starting from the so-call variation of constants formulae and applying the same quadrature rules as in the DI case, the ETD integrators are obtained. This approach allows one to directly compare a DI

integrator with its ETD counterpart. Additionally, the accuracy of each integrator is discussed and the stability conditions of the resulting FDTD schemes are derived in exact closed-form.

## II. GOVERNING EQUATIONS

The time-dependent Maxwell curl equations in linear, isotropic, electrically dispersive media can be expressed as

$$\mu \frac{\partial \vec{H}}{\partial t} = -\nabla \times \vec{E}, \quad \varepsilon \frac{\partial \vec{E}}{\partial t} = \nabla \times \vec{H} - \vec{J}, \quad (1)$$

where  $\mu$  is the permeability and  $\varepsilon$  is the permittivity. In the frequency domain, the current density is related to the electric field by the constitutive relation

$$\vec{J}(\omega) = \sigma(\omega) \vec{E}(\omega) = \frac{\sigma_S}{1 + j\omega\tau} \vec{E}(\omega), \quad (2)$$

where a Drude dispersion model has been assumed for the conductivity function  $\sigma(\omega)$ . In (2),  $\sigma_S$  is the static conductivity and  $\tau$  is the relaxation time constant. For  $\tau = 0$ , the Drude model reduces to a simple static conductivity.

Considering the transformation  $j\omega \leftrightarrow d/dt$ , (2) can be expressed in the time domain as a first-order ordinary differential equation (ODE):

$$\tau \frac{d\vec{J}}{dt} + \vec{J} = \sigma_S \vec{E}. \quad (3)$$

In the next section, we address the discretization of (3) by using DI and ETD methods.

## III. CONSTITUTIVE RELATION INTEGRATORS

### A. DI integrators

Integrating (3) over a single time step from  $t_n = n\Delta_t$  to  $t_{n+1} = (n+1)\Delta_t$ , we have

$$\vec{J}^{n+1} = \vec{J}^n - \frac{1}{\tau} \int_{t_n}^{t_{n+1}} \vec{J}(t) dt + \frac{\sigma_S}{\tau} \int_{t_n}^{t_{n+1}} \vec{E}(t) dt. \quad (4)$$

Then, approximating  $\vec{J}(t)$  within the integrating interval by a first-degree polynomial as

$$\vec{J}(t) \simeq \vec{J}^n + \frac{\vec{J}^{n+1} - \vec{J}^n}{\Delta_t} (t - t_n), \quad (5)$$

the following general expression is obtained

$$\vec{J}^{n+1} = \vec{J}^n - \frac{\Delta_t}{2\tau} (\vec{J}^{n+1} + \vec{J}^n) + \frac{\sigma_S}{\tau} \int_{t_n}^{t_{n+1}} \vec{E}(t) dt. \quad (6)$$

Different numerical integrators can now be obtained by applying quadrature rules to approximate the integral in (6). The simplest approximation consists of assuming  $\vec{E}$  to be a constant over the integrating interval. For instance, the choice  $\vec{E}(t) \simeq \vec{E}^n$  leads to the explicit-Euler (EE)-DI scheme that reads

$$\vec{J}^{n+1} = a_1 \vec{J}^n + a_2 \vec{E}^n, \quad (7)$$

Manuscript received December 21, 2021. This work is part of the I+D+i projects PGC2018-098350-B-C21 and PGC2018-098350-B-C22, supported by MCIN/AEI/10.13039/501100011033/FEDER “Una manera de hacer Europa”.

J. A. Pereda is with the Dpto. de Ingeniería de Comunicaciones (DICOM), Universidad de Cantabria, Edificio Ingeniería de Telecomunicación, Plaza de la Ciencia s/n, 39005 Santander, Cantabria, Spain (email: peredaj@unican.es).

A. Grande is with the Dpto. de Electricidad y Electrónica, Universidad de Valladolid, 47011 Valladolid, Spain (email: agrande@uva.es).

where

$$a_1 = \frac{2\tau - \Delta_t}{2\tau + \Delta_t}, \quad a_2 = \frac{2\sigma_S \Delta_t}{2\tau + \Delta_t}. \quad (8)$$

Instead, by letting  $\vec{E}(t) \simeq \vec{E}^{n+1}$  in (6), the following implicit-Euler (IE)-DI integrator is obtained:

$$\vec{J}^{n+1} = a_1 \vec{J}^n + a_2 \vec{E}^{n+1}. \quad (9)$$

This scheme has recently been used to model graphene's intraband conductivity [15].

Additionally, the choice  $\vec{E}(t) \simeq \vec{E}^{n+\frac{1}{2}}$  in (6) leads to the midpoint (MP)-DI scheme:

$$\vec{J}^{n+1} = a_1 \vec{J}^n + a_2 \vec{E}^{n+\frac{1}{2}}, \quad (10)$$

which was introduced in [14] to simulate isotropic plasma and adopted in [16] to model graphene's intraband conductivity.

To improve the integration accuracy in (6),  $\vec{E}(t)$  is linearly interpolated within the integrating interval, analogously to (5). As a result, the trapezoidal (TR)-DI scheme is obtained:

$$\vec{J}^{n+1} = a_1 \vec{J}^n + \frac{a_2}{2} (\vec{E}^{n+1} + \vec{E}^n). \quad (11)$$

An alternative approach to obtain (11) consists of averaging the electric field in (10) as  $E^{n+\frac{1}{2}} \simeq (\vec{E}^{n+1} + \vec{E}^n)/2$ . This scheme can also be derived by applying the Mobius (bilinear) transformation method to the frequency-domain  $J$ - $E$  constitutive relation (2), as was shown in [9]. For cold plasma, (11) is the same as the "new DI method" introduced in [5].

### B. ETD integrators

Multiplying (3) by  $e^{t/\tau}$  and noting that the left-hand side of the resulting equation is the derivative of a product, we can write

$$\frac{d}{dt} (e^{t/\tau} \vec{J}) = \frac{\sigma_S}{\tau} e^{t/\tau} \vec{E}. \quad (12)$$

The variation of constants formulae is obtained by integrating (12) from  $t_n = n\Delta_t$  to  $t_{n+1} = (n+1)\Delta_t$  as

$$\vec{J}^{n+1} = e^{-\Delta_t/\tau} \vec{J}^n + \frac{\sigma_S}{\tau} \int_{t_n}^{t_{n+1}} e^{(t-t_{n+1})/\tau} \vec{E}(t) dt. \quad (13)$$

Note that (13) is the exact solution to (3) with initial condition  $\vec{J}(t_n) = \vec{J}^n$ . The approach now runs parallel to the one applied for the DI integrators: first  $\vec{E}(t)$  in (13) is replaced by a Newton interpolation polynomial and the resulting integral is then solved exactly. Specifically, letting  $\vec{E}(t) \simeq \vec{E}^n$ ,  $\vec{E}(t) \simeq \vec{E}^{n+1}$  and  $\vec{E}(t) \simeq \vec{E}^{n+\frac{1}{2}}$  in (13), the EE-ETD

$$\vec{J}^{n+1} = b_1 \vec{J}^n + b_2 \vec{E}^n, \quad (14)$$

IE-ETD

$$\vec{J}^{n+1} = b_1 \vec{J}^n + b_2 \vec{E}^{n+1} \quad (15)$$

and MP-ETD

$$\vec{J}^{n+1} = b_1 \vec{J}^n + b_2 \vec{E}^{n+\frac{1}{2}} \quad (16)$$

integrators are respectively obtained, where

$$b_1 = e^{-\Delta_t/\tau}, \quad b_2 = \sigma_S \left(1 - e^{-\Delta_t/\tau}\right). \quad (17)$$

The IE-ETD scheme was used in [17] and the MP-ETD method in [18] and [19]. In all the cases for plasma modeling,

Analogously, approximating  $\vec{E}(t)$  in (13) by a first-degree polynomial, the TR-ETD integrator is obtained as

$$\vec{J}^{n+1} = b_1 \vec{J}^n + b_2 \vec{E}^n + \sigma_S \left( \frac{e^{-\Delta_t/\tau} - 1}{\Delta_t/\tau} + 1 \right) (\vec{E}^{n+1} - \vec{E}^n). \quad (18)$$

This scheme has been used for modeling plasma and graphene in [5] and [20], respectively.

An additional ETD scheme can be obtained by averaging  $\vec{E}^{n+\frac{1}{2}}$  in (16) as

$$\vec{J}^{n+1} = b_1 \vec{J}^n + \frac{b_2}{2} (\vec{E}^{n+1} + \vec{E}^n). \quad (19)$$

This scheme was used in [21] for magnetized plasma. We will refer to it as the averaged (A)MP-ETD integrator.

It is worth noting that replacing the exponential function by the Padé approximant

$$e^{-\Delta_t/\tau} = \frac{1 - \frac{\Delta_t}{2\tau}}{1 + \frac{\Delta_t}{2\tau}} + O[(\Delta_t/\tau)^3], \quad (20)$$

any of the above ETD integrators leads to its DI counterpart. Hence, DI and ETD schemes are equivalent for  $\Delta_t \ll \tau$ .

### C. Integrators accuracy

To illustrate the order of accuracy of the integrators introduced above, we consider an example consisting of the integration of the  $x$ -component of (3) with a known forcing function  $E_x(t) = E_0 \sin(\omega t + \phi)$  and an initial condition  $J_x(0) = 0$ . Under these conditions, the exact solution to the current density is

$$J_{x,\text{exa.}}(t) = \frac{E_0}{(\omega\tau)^2 + 1} [\sin(\omega t + \phi) - \tau\omega \cos(\omega t + \phi)] - \frac{E_0\sigma_S}{(\omega\tau)^2 + 1} (\sin\phi - \tau\omega \cos\phi) e^{-t/\tau}. \quad (21)$$

The numerical current density,  $J_{x,\text{num.}}$ , has been calculated along the first wave period  $T = 2\pi/\omega$  by using a time step  $\Delta_t = T/N_t$ , where  $N_t$  is the time resolution. The data used were  $E_0 = 1$  V/m,  $\omega = 2\pi \times 10^{11}$  rad/s,  $\phi = 0$ ,  $\sigma_S = 100$  S/m and  $\tau = 0.5$  ps. Fig. 1 depicts the RMS error defined as

$$\mathcal{E}_{\text{RMS}} = \frac{1}{N_t} \left( \sum_{n=1}^{N_t} |J_{x,\text{exa.}}^n - J_{x,\text{num.}}^n|^2 \right)^{\frac{1}{2}} \quad (22)$$

against the time resolution  $N_t$ . For the two families of integrators, it can be seen that the MP and the TR schemes have second-order accuracy. The AMP-ETD scheme has second-order accuracy, as well. However, the Euler schemes are first-order accurate only.

In the next section we address the coupling of the DI and ETD integrators to the FDTD Maxwell equations.

## IV. FDTD SCHEMES

### A. Time-located $J$ - $E$ and $J$ - $H$ formulations

According to the conventional FDTD method [1], Faraday's equation in (1) is approximated at  $t = n\Delta_t$  as

$$\vec{H}^{n+\frac{1}{2}} = \vec{H}^{n-\frac{1}{2}} - \frac{\Delta_t}{\mu} \nabla \times \vec{E}^n. \quad (23)$$

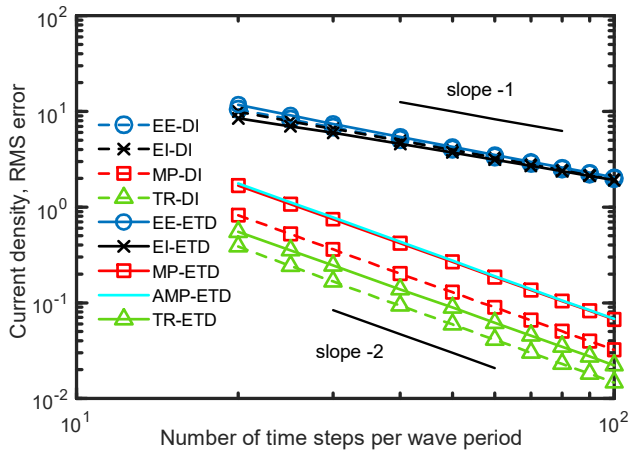


Fig. 1. Current density RMS error versus the number of time steps per period for several DI and ETD integrators.

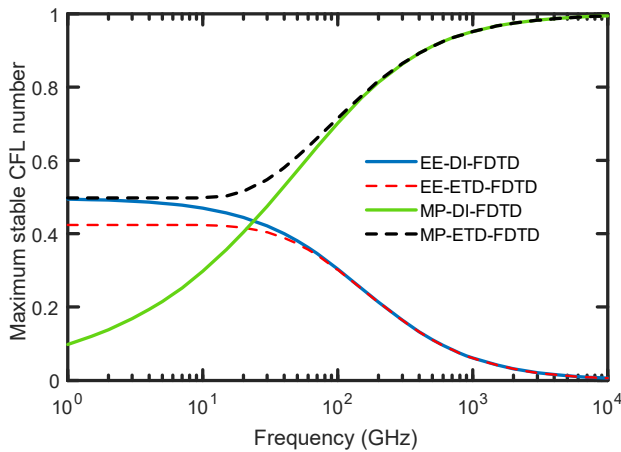


Fig. 2. Maximum stable CFL number  $\nu_{\max}$  versus frequency for explicit DI- and ETD-FDTD schemes.

Analogously, Ampère's law is discretized at  $t = (n + \frac{1}{2})\Delta t$  as

$$\vec{E}^{n+1} = \vec{E}^{n+1} + \frac{\Delta t}{\epsilon} \nabla \times \vec{H}^{n+\frac{1}{2}} - \frac{\Delta t}{\epsilon} \vec{J}^{n+\frac{1}{2}}. \quad (24)$$

Averaging the current density in (24), the following alternative discretization to Ampère's equation is obtained

$$\vec{E}^{n+1} = \vec{E}^{n+1} + \frac{\Delta t}{\epsilon} \nabla \times \vec{H}^{n+\frac{1}{2}} - \frac{\Delta t}{2\epsilon} (\vec{J}^{n+1} + \vec{J}^n). \quad (25)$$

We will refer to (24) and (25) as time-located  $J$ - $H$  and  $J$ - $E$  formulations, respectively. The same spatial discretization as in the conventional FDTD method is assumed in (23)-(25), [1].

In order to incorporate Drude media into FDTD simulations, the Euler, TR and AMP-ETD integrators are coupled to (25) since they are time-located  $J$ - $E$  schemes, as well. On the other hand, the MP integrators are time-located  $J$ - $H$  schemes that should be used jointly with (24). To this end, (10) and (16) are shifted by a half time step.

## B. Stability

To study the stability of the FDTD schemes outlined above, we adopt the von Neumann method, according to the procedure given in [22] and [9]. Derivation details are omitted for the sake of brevity.

We have found that the FDTD schemes based on implicit integrators preserve the stability limit of the conventional FDTD method. However, this is not the case for the FDTD schemes based on explicit integrators, as specified as follows.

For the EE-DI-FDTD scheme the stability condition reads

$$\nu \leq \nu_{\max} = \sqrt{(A+B)^2 + 1} - (A+B), \quad (26)$$

where  $\nu = \Delta t / \Delta_{t,\max}^{\text{CFL}}$  is the Courant–Friedrichs–Lewy (CFL) number,  $\Delta_{t,\max}^{\text{CFL}}$  is the largest stable time step permitted by the conventional FDTD method, given by [1]

$$\Delta_{t,\max}^{\text{CFL}} = \sqrt{\epsilon\mu} \left( \frac{1}{\Delta_x^2} + \frac{1}{\Delta_y^2} + \frac{1}{\Delta_z^2} \right)^{-\frac{1}{2}} \quad (27)$$

and

$$A = \frac{\tau}{\Delta_{t,\max}^{\text{CFL}}}, \quad B = \frac{\sigma_S \Delta_{t,\max}^{\text{CFL}}}{4\epsilon}. \quad (28)$$

For  $\tau = 0$ , (26) agrees with the stability condition of the time-backward differencing scheme for the FDTD method in lossy media [13].

For the MP-DI-FDTD method we have

$$\nu \leq \nu_{\max} = \frac{1}{\sqrt{1+B/A}}. \quad (29)$$

This condition was previously derived in [14] and [15].

For the EE-ETD- and the MP-ETD-FDTD schemes, the stability conditions are, respectively,

$$\nu \leq \nu_{\max} = \sqrt{(BC)^2 + C} - BC \quad (30)$$

and

$$\nu \leq \nu_{\max} = \sqrt{\left(\frac{BC}{D}\right)^2 + 1} - \frac{BC}{D}, \quad (31)$$

with  $C = (1 - e^{-\Delta t/\tau})/2$  and  $D = (1 + e^{-\Delta t/\tau})/2$ . To the best of our knowledge, the stability conditions for the EE-DI-, EE-ETD- and MP-ETD-FDTD methods given in (26), (30) and (31), respectively, are herein reported in exact closed-form for the first time. It is worth noting, however, that (30) and (31) are implicit expressions of the time step. Thus, an iterative process needs to be performed to obtain the maximum stable time step.

To illustrate the implications of the above stability expressions, we consider the 1D-FDTD simulation of a monochromatic plane wave propagating in free-space along the  $z$ -direction and impinging normally on an infinite graphene sheet. The spatial step is  $\Delta_z = \lambda_0/40$ , where  $\lambda_0$  is the wavelength in free-space. The graphene parameters are  $\tau = 0.184$  ps and  $\sigma_S = \sigma_0/\Delta_z$ , with  $\sigma_0 = 8$  mS. These parameters have been taken from [23]. For this problem  $\Delta_{t,\max}^{\text{CFL}} = \sqrt{\epsilon_0\mu_0}\Delta_z$ . Fig. 2 depicts the maximum stable CFL number  $\nu_{\max}$ , calculated by (26) and (29)-(31), versus the wave frequency in the band  $[1 - 10^4]$  GHz. Note that the parameter  $\Delta_{t,\max}^{\text{CFL}}/\tau$  varies

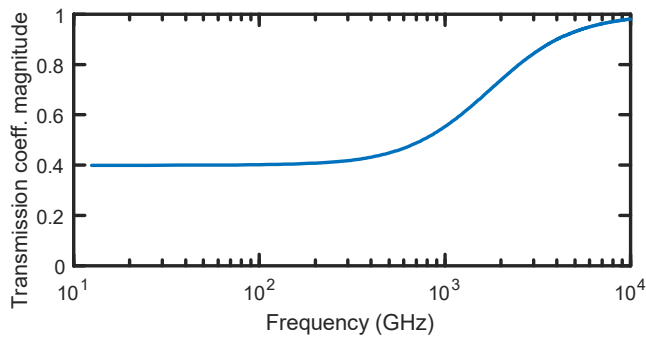


Fig. 3. Exact transmission coefficient magnitude versus frequency.

accordingly in the range  $[140 - 0.014]$ . It can be seen that, in general, all the explicit schemes suffer from very severe stability restrictions. Only under the condition  $\Delta_t/\tau < 1$ , the MP formulations have a value of  $\nu_{\max}$  approaching unity.

### C. Simulation examples

We consider the calculation of the transmission coefficient of a plane wave propagating in free-space and impinging normally on an infinite graphene sheet. Fig. 3 plots the exact solution to this example given by  $\mathcal{T}_{\text{exa.}} = 2/(2 + \eta_0 \sigma_g)$  [24], where  $\eta_0 = \sqrt{\mu_0/\epsilon_0}$  and  $\sigma_g = \sigma_0/(1 + j\omega\tau)$  is the superficial graphene's conductivity. We have used the same values of  $\sigma_0$  and  $\tau$  as in Fig. 2. We now consider the FDTD simulation of this problem by using an incident Gaussian pulse under two different conditions.

Firstly, the maximum effective frequency of the Gaussian pulse is assumed to be  $f_{\max} = 10$  GHz. The spatial step is  $\Delta_z = \lambda_{\min}/40$ , where  $\lambda_{\min}$  is the minimum wavelength in free-space, i.e.  $\lambda_{\min} = 1/(\sqrt{\epsilon_0\mu_0}f_{\max})$ . Fig. 4 plots the absolute error of the transmission coefficient magnitude,  $\mathcal{E}_{\text{abs}} = |\mathcal{T}_{\text{exa.}}| - |\mathcal{T}_{\text{FDTD}}|$ , as a function of frequency for all the second-order accurate methods. For each method, the simulation has been carried out with its maximum stable time step. Although it is widely assumed that DI methods fail unless  $\Delta_t/\tau \ll 1$ , results in Fig. 4, obtained for  $\Delta_{t,\max}^{\text{CFL}}/\tau \simeq 14$ , show that both DI and ETD methods provide good accuracy and exhibit quite close performance also for  $\Delta_t/\tau > 1$ . This agrees with the conclusions drawn in [12] for lossy and plasma media. It can be also seen in Fig.4 that the TR-DI-FDTD scheme is the most accurate method in this example.

Secondly, the simulation is carried out in the whole frequency band, i.e.  $f_{\max} = 10$  THz. Again, the spatial step is  $\Delta_z = \lambda_{\min}/40$  and the maximum stable time step for each scheme is considered. In this case, we have  $\Delta_{t,\max}^{\text{CFL}}/\tau \simeq 0.014$ . Fig. 5 depicts the absolute error of the transmission coefficient magnitude against frequency for the same methods as in Fig. 4. Again, similar accuracy is observed for DI and ETD methods.

## V. CONCLUSION

A unified view of DI and ETD methods for Drude media has been provided. It has been shown that FDTD schemes based on implicit DI and ETD integrators preserve the stability

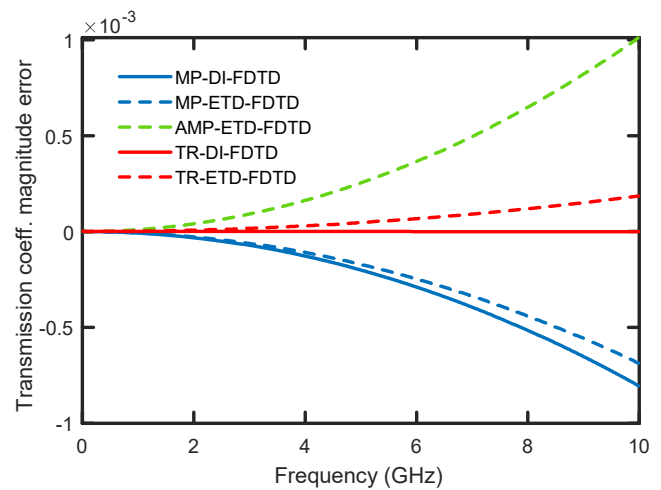


Fig. 4. Absolute error of the transmission coefficient magnitude versus frequency.  $\Delta_{t,\max}^{\text{CFL}}/\tau \simeq 14$ .

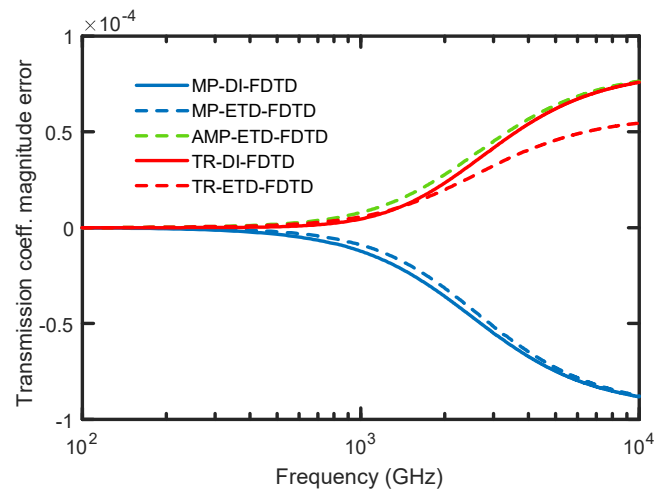


Fig. 5. Absolute error of the transmission coefficient magnitude versus frequency.  $\Delta_{t,\max}^{\text{CFL}}/\tau \simeq 0.014$ .

limit of the conventional FDTD method. However, FDTD schemes based on explicit integrators may suffer from very severe stability restrictions. The FDTD simulation examples have shown that DI- and ETD-FDTD methods exhibit similar accuracy despite the value of  $\Delta_t/\tau$ . The methodology outlined in this communication can also be applied to higher-order dispersive media by expressing their constitutive relation as a system of first-order ODEs.

## REFERENCES

- [1] A. Taflove and S. C. Hagness, *Computational Electrodynamics: The Finite-Difference Time-Domain Method*, 3rd ed. Norwood, MA: Artech House, 2005.
- [2] T. Kashiwa and I. Fukai, "A treatment by the FDTD method of the dispersive characteristics associated with electronic polarization," *Microwave Opt. Technol. Lett.*, vol. 3, pp. 203–205, Jun. 1990.
- [3] R. M. Joshep, S. C. Hagness, and A. Taflove, "Direct time integration of Maxwell's equations in linear dispersive media with absorption for scattering and propagation of femtosecond electromagnetic pulses," *Opt. Lett.*, vol. 16, pp. 1412–1414, Sept. 1991.

- [4] D. F. Kelly and R. J. Luebbers, "Piecewise linear recursive convolution for dispersive media using FDTD," *IEEE Trans. Antennas Propag.*, vol. 44, pp. 792–797, Jun. 1996.
- [5] S. A. Cummer, "An analysis of new and existing FDTD methods for isotropic cold plasma and a method for improving their accuracy," *IEEE Trans. Antennas Propag.*, vol. 45, pp. 392–400, Mar. 1997.
- [6] Q. Chen, M. Katsuari, and P. H. Aoyagi, "An FDTD formulation for dispersive media using a current density," *IEEE Trans. Antennas Propag.*, vol. 46, pp. 1739–1746, Oct. 1998.
- [7] D. Y. Heh and E. L. Tan, "FDTD modeling for dispersive media using matrix exponential method," *IEEE Microw. Wireless Compon. Lett.*, vol. 19, no. 2, pp. 53–55, Feb. 2009.
- [8] D. M. Sullivan, "Z-transform theory and the FDTD method," *IEEE Trans. Antennas Propag.*, vol. 44, pp. 28–34, Jan. 1996.
- [9] J. A. Pereda, A. Vegas, and A. Prieto, "FDTD modeling of wave propagation in dispersive media by using the Mobius transformation technique," *IEEE Trans. Microw. Theory Techn.*, vol. 50, pp. 1689–1695, Jul. 2002.
- [10] B. V. Minchev and W. M. Wright, *A review of exponential integrators for first order semi-linear problems*, Tech. report 2/05, Department of Mathematics, NTNU, 2005.
- [11] J. L. Young and R. G. Nelson, "A summary of systematic analysis of FDTD algorithms for linearly dispersive media," *IEEE Antennas Propag. Mag.*, vol. 43, no. 1, pp. 61–126, Feb. 2001.
- [12] J.-P. Bérenger, "Comparison of the standard differencing with the exponential differencing for the FDTD method in lossy media," *IEEE J. Multiscale Multiphys. Comput. Techn.*, vol. 3, pp. 295–302, 2018.
- [13] L. F. Velarde, J. A. Pereda, A. Vegas and O. Gonzalez, "A weighted-average scheme for accurate FDTD modeling of electromagnetic wave propagation in conductive media", *IEEE Antennas Wireless Propag. Lett.*, vol. 3, pp. 302–305, 2004.
- [14] J. L. Young, "A full finite difference time domain implementation for radio wave propagation in a plasma," *Radio Science*, vol. 29, pp. 1513–1522, 1994.
- [15] O. Ramadan, "Improved direct integration auxiliary differential equation FDTD scheme for modeling graphene drude dispersion," *Optik*, vol. 219, 165173, Oct. 2020.
- [16] D. Bouzianas, N. Kantartzis, S. Antonopoulos, and T. Tsiiboukis, "Optimal modeling of infinite graphene sheets via a class of generalized FDTD schemes," *IEEE Trans. Magn.*, vol. 48, no. 2, pp. 379–382, Feb. 2012.
- [17] H. Yang, "Exponential FDTD for plasma dispersive medium," *J. of Electromagn. Waves and Appl.*, vol. 22, pp. 1165–1172, 2008.
- [18] M. Thévenot, J.-P. Bérenger, T. Monédière, and F. Jecko, "A FDTD scheme for the computation of VLF-LF propagation in the anisotropic earth-ionosphere waveguide," *Ann. Telecommun.*, vol. 54, nos. 5–6, pp. 297–310, 1999.
- [19] Sh. J. Huang, "Exponential time differencing FDTD formulation for plasma," *Microw. Opt. Technol. Lett.*, vol. 49, pp. 1363–1364, Jun. 2007.
- [20] O. Ramadan, "Runge-Kutta exponential time differencing scheme for incorporating graphene dispersion in the FDTD simulations," *Progress In Electromagnetics Research Lett.*, Vol. 84, pp. 15–21, 2019.
- [21] J.-P. Bérenger, "An implicit FDTD scheme for the propagation of VLF-LF radio waves in the earth-ionosphere waveguide," *Comptes Rendus Physique*, vol. 15, pp. 393–402, 2014.
- [22] J. A. Pereda, L. A. Vielva, A. Vegas, and A. Prieto, "Analyzing the stability of the FDTD technique by combining the von Neumann method with the Routh-Hurwitz criterion," *IEEE Trans. Microw. Theory Techn.*, vol. 49, no. 2, pp. 377–381, Feb. 2001.
- [23] D. Sounas and C. Caloz, "Gyrotropy and nonreciprocity of graphene for microwave applications", *IEEE Trans. Microw. Theory Techn.*, vol. 60, no. 4, pp. 901–914, Apr. 2012.
- [24] G. Hanson, "Dyadic green's functions and guided surface waves for a surface conductivity model of graphene," *J. Appl. Phys.*, vol. 103, 064302, 2008.